

and D. M. Yuden, *Phys. Status Solidi* **2**, 865 (1970).

¹⁹A. J. Bennett, B. McCarroll, and R. P. Messmer, *Surface Sci.* **24**, 191 (1971).

²⁰A. J. Bennett, B. McCarroll, and R. P. Messmer, *Phys. Rev. B* **3**, 1397 (1971).

²¹A. J. Bennett and L. M. Roth, *J. Phys. Chem. Solids* **32**, 1251 (1971); L. M. Roth and A. J. Bennett, in *Proceedings of the Tenth International Conference on the Physics of Semiconductors, Cambridge, Mass., 1970* (U.S. AEC, Oak Ridge, 1970), p. 619.

²²R. P. Messmer and G. D. Watkins, *Phys. Rev. Letters* **25**, 656 (1970).

²³R. W. G. Wyckoff, *Crystal Structures*, Vol. 1 (Interscience, N. Y., 1963).

²⁴J. Stuke, *J. Non-Cryst. Solids* **4**, 1 (1970).

²⁵M. H. Brodsky and R. S. Title, *Phys. Rev. Letters* **23**, 581 (1969).

²⁶R. Hoffman, *J. Chem. Phys.* **36**, 2179 (1962); **36**, 2189 (1962); **40**, 2474 (1963).

²⁷K. Jug, *Theoret. Chim. Acta (Berlin)* **14**, 91 (1969).

²⁸T. M. Donovan and W. E. Spicer, *Phys. Rev. Letters* **21**, 1572 (1968).

²⁹T. L. Gilbert, in *Sigma Molecular Orbital Theory*, edited by O. Sinanoglú and K. B. Wiberg (Benjamin, New York, 1969), p. 249.

³⁰L. C. Allen, in Ref. 29, p. 227.

³¹F. Herman and S. Skillman, *Atomic Structure Calculations* (Prentice-Hall, Englewood Cliffs, N. J., 1963).

³²C. E. Moore, *Natl. Bur. Std. (U. S.) Arch. No. 467* (1949) (unpublished).

³³D. P. Santry and G. A. Segal, *J. Chem. Phys.* **47**, 158 (1967); J. A. Pople and G. A. Segal, *ibid.* **43**, 5136 (1965).

³⁴D. W. J. Cruickshank, *J. Chem. Soc.* 5486 (1961).

³⁵F. Bassani and M. Yoshimine, *Phys. Rev.* **130**, 20 (1963).

³⁶See, e. g., M. L. Cohen and T. K. Bergstresser, *Phys. Rev.* **141**, 789 (1966), and references therein.

³⁷R. P. Messmer (unpublished).

³⁸R. C. Chaney, C. C. Lin, and E. E. Lafon, *Phys. Rev. B* **3**, 459 (1971).

Effect of Pressure on the Static Dielectric Constant of KTaO_3 [†]

W. R. Abel

Sandia Laboratories, Albuquerque, New Mexico 87115

(Received 27 May 1971)

The static dielectric constant ϵ of KTaO_3 has been measured from 4 to 300 K and at pressures up to 26 kbar. The temperature T_1 at which ϵ deviates from a Curie-Weiss law, attributed to quantum effects, is found to increase with increasing pressure with a slope $d \ln T_1 / dP = 3\%/\text{kbar}$. At zero pressure, T_1 is 53 K. The pressure dependences of the Curie constant and Curie temperature were obtained also. The Curie constant decreases at the rate of 0.9%/kbar, and the Curie temperature decreases at the rate of 4.8 K/kbar. The reason for the increase of T_1 with pressure is discussed.

INTRODUCTION

It has long been known that ferroelectrics with very low Curie temperatures show deviations from the Curie-Weiss law for their dielectric response at temperatures much greater than the Curie temperature.^{1,2} As the temperature of a paraelectric sample is lowered, a temperature (defined as T_1) is reached below which the static dielectric constant ϵ changes less rapidly than predicted by $\epsilon = B/(T - T_0)$. At temperatures much less than T_1 , ϵ becomes temperature independent. A more precise definition of T_1 will be used later, but it is, in effect, the temperature at which the Curie-Weiss law fails. SrTiO_3 and KTaO_3 are examples of materials which exhibit this behavior. They both have a T_0 below 35 K, and start deviating from the Curie-Weiss law at a temperature of about 50 K. This behavior is usually attributed to quantum effects. Slater treated an ion in an anharmonic potential well classically in order to derive the

ionic polarizability of a ferroelectric crystal in its paraelectric phase.³ In 1952, J. H. Barrett⁴ extended this theory by carrying out a quantum-mechanical treatment of the ionic polarizability. In his theory, the lowest quantum level for the ion has an energy equal to kT_1 , so that for temperatures less than T_1 all ions are in their lowest energy states and further reduction in the temperature causes no change in the dielectric response. Barrett derived the relation

$$\epsilon = B / \left[\frac{1}{2} T_1 \coth(T_1/2T) - T_0 \right], \quad (1)$$

and this seems to fit experiments quite well, if T_1 , T_0 , and B are treated as empirically determined constants. Barrett was not successful in determining these constants from first principles.

Pressure experiments have been made on many ferroelectrics in order to find the volume dependence of T_0 and the Curie constant B , effects which are now fairly well understood.⁵ However, apparently no study of the volume dependence of T_1

has been undertaken. We have measured the dielectric constant of KTaO_3 from 4–300 K and 0–26 kbar, in order to find the dependence of T_1 on pressure. The pressure dependences of B and T_0 for KTaO_3 were obtained as well. KTaO_3 was chosen because it undergoes no phase transition and remains paraelectric to 4 K. The series of (nonferroelectric) phase transitions in SrTiO_3 at low temperatures could possibly make measurements on this substance more difficult to interpret. Dielectric anisotropies which depend on the conditions under which the sample is cooled have been observed for SrTiO_3 .⁶

EXPERIMENTAL TECHNIQUE

Measurements were made on two single-crystal samples from the same boule,⁷ one in a piston-cylinder cell and one in a helium-gas bomb. Each

sample was about 1.3 mm thick and 7 mm diam and had aluminum electrodes evaporated on each face. The capacities of the samples were measured by means of a three-terminal technique with a General Radio type 1615A capacitance bridge, using a measuring frequency of 100 kHz. The frequency dependence of the sample capacity was checked at room temperature and found to be negligible. The samples had very low conductivities; the loss factors were less than 0.01 at 100 kHz.

The first sample was completely surrounded by AgCl , which served as the pressure transmitting medium, and loaded into a 9.5-mm-diam piston-cylinder pressure cell, with care being taken to keep all tolerances very close in order to minimize nonhydrostatic stress. Thin copper tabs were used to put the sample faces into electrical contact with

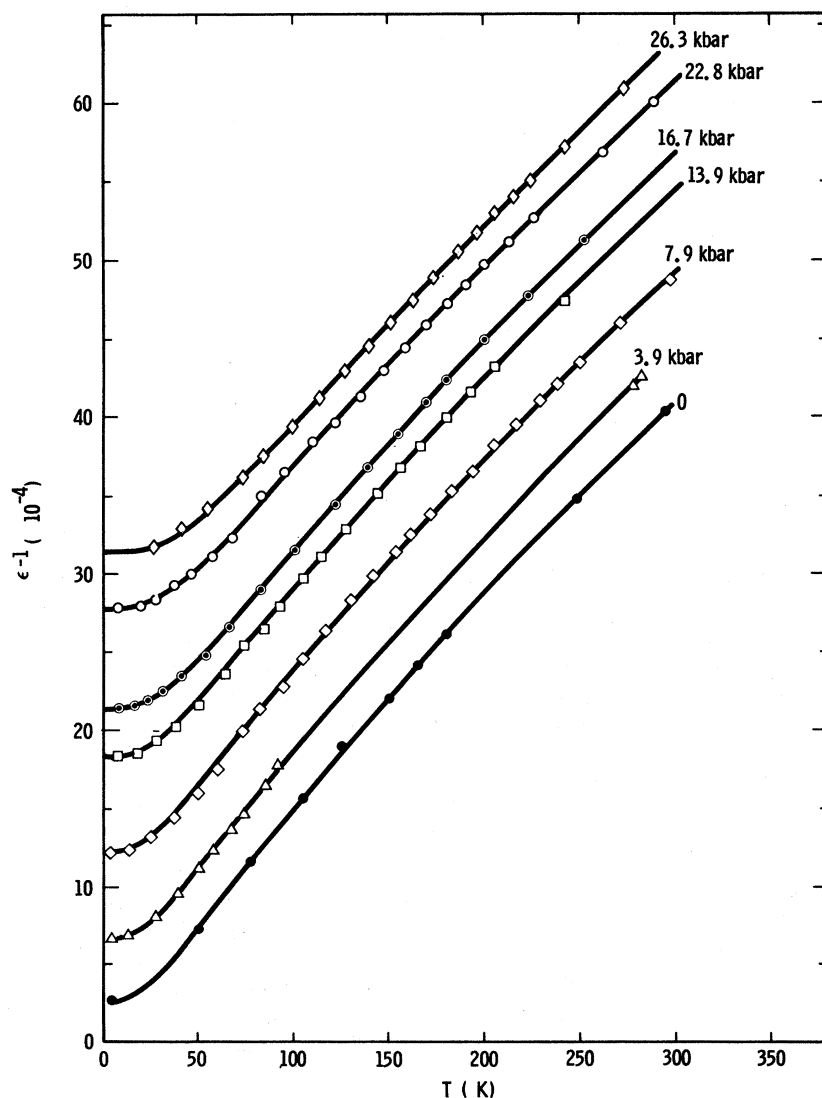


FIG. 1. Inverse dielectric constant ϵ^{-1} vs temperature at various pressures. The zero-pressure data were obtained from sample II. All others were from sample I. The solid lines are fits of the expression $\epsilon = A + B / [\frac{1}{2}T_1 \coth(T_1/2T) - T_0]$.

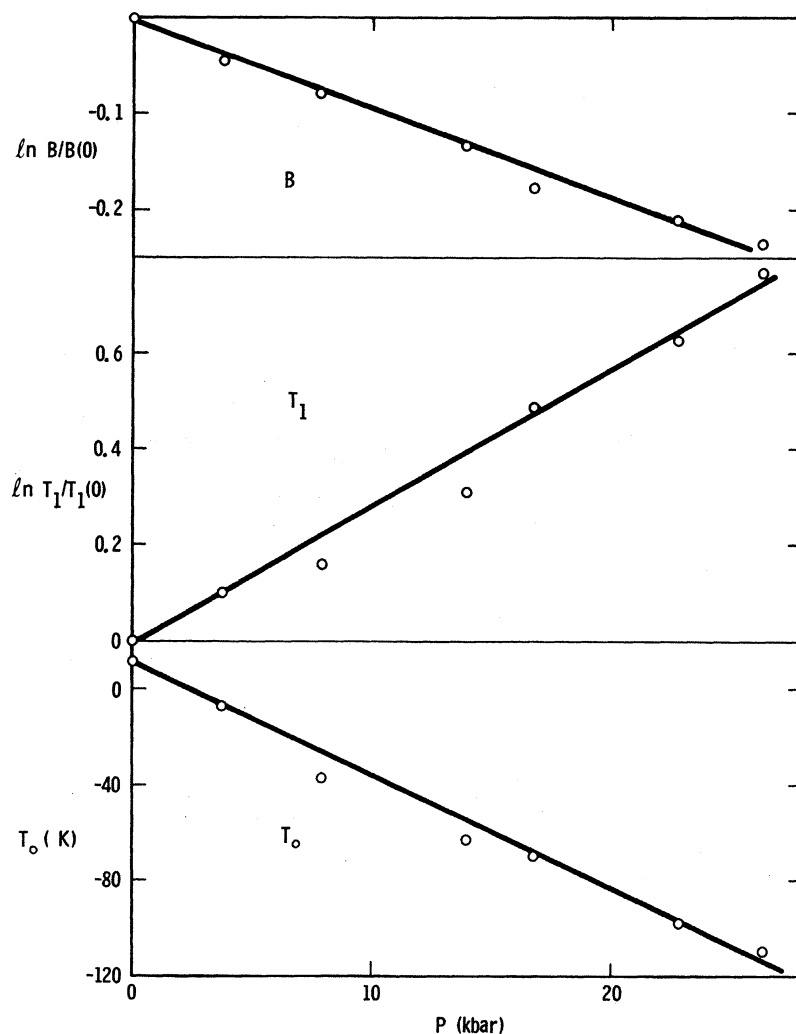


FIG. 2. Parameters used to fit the data shown in Fig. 1 as a function of pressure.

the two pistons, which were insulated from the cylinder with mica and used as electrical leads. This piston-cylinder cell was then placed in a high-pressure cryostat similar to one described by Lyon *et al.*⁸ The cell was cooled to 4 K while a constant load was maintained on the pistons. The load was measured by a strain-gauge load cell. The capacity was then measured as a function of temperature as the device warmed, still at constant load. Pressure was assumed to be proportional to the load. The constant of proportionality was determined from measurements of the Bi I-II transition in a similar piston-cylinder apparatus. The pressure thus obtained is probably accurate to $\pm 5\%$, although the precision with which the load was held constant during a given run was much greater than this. Pressure was changed only at temperatures greater than 270 K, to keep it as hydrostatic as possible. A total of six runs was made, at pressures ranging from 3.8 to 26.3 kbar. Temperatures were measured using Cu-

constantan thermocouples above 40 K and Cu-AuFe thermocouples below 40 K. Both thermocouples were calibrated against platinum and germanium resistance thermometers. The results are shown in Fig. 1.

The second sample was loaded into a BeCu pressure bomb, and the capacitance was measured as a function of pressure with the temperature held constant. Helium gas was used as a pressure transmitting medium. The He pressurizing device was made after a design by Schirber.⁹ Several runs were made, holding the temperature constant at temperatures ranging from 50 K to room temperature. Measurements at 4 K were made after pressurizing at temperatures above the helium freezing temperature and then freezing the helium from the bottom of the bomb up, under constant pressure. For each pressure at 4 K, the bomb was warmed and this procedure repeated. We were able to get reproducible results provided the cooling rate was kept sufficiently slow. Pres-

TABLE I. Pressure derivatives of the parameters B , T_1 , and T_0 for KTaO_3 . These parameters are defined in the text. Their values at 1 bar are $B=5.52 \times 10^4$ K, $T_0=11.8$ K, and $T_1=53.3$ K.

	Sample I (piston and cylinder apparatus)	Sample II (helium-gas bomb)
$\frac{d \ln B}{dP}$	$(-0.92 \pm 0.05)\%/kbar$	$(-0.81 \pm 0.05)\%/kbar$
$\frac{dT_0}{dP}$	$(-4.8 \pm 0.2) K/kbar$	$(-4.6 \pm 0.2) K/kbar$
$\frac{dT_1}{dP}$	$(1.49 \pm 0.05) K/kbar^a$	$(1.9 \pm 0.3) K/kbar$
$\frac{d \ln T_1}{dP}$	$(2.8 \pm 0.1)\%/kbar$	$(3.5 \pm 0.6)\%/kbar$

^aInitial value, for comparison with sample II. The value of dT_1/dP is not constant over the range of pressures under which sample I was measured.

sure was measured using a Heise gauge. Pressures for the 4-K data were corrected for effects of the thermal contraction of the solid helium by using the data of Dugdale.¹⁰ Temperatures for all runs except the 4-K isotherm were measured using Cu-constantan thermocouples. The lowest temperature run was made in liquid He at a vapor

pressure of 620 mm Hg.

RESULTS AND DISCUSSION

It was found that the data from each run on sample I and the zero-pressure data on sample II could be fitted to the following expression:

$$\epsilon = A + B / \left[\frac{1}{2} T_1 \coth(T_1/2T) - T_0 \right] \quad (2)$$

The parameter A is the temperature-independent contribution to the polarizability and is small but nonnegligible in KTaO_3 . It is 48.3 and independent of pressure, at least within experimental error. B , T_1 , and T_0 all depend on pressure. These parameters are plotted vs pressure in Fig. 2. The zero-pressure values are in good agreement with the dielectric constant measurements of Wemple.¹¹ From the plots of B , T_1 , and T_0 the derivatives $d \ln B/dP$, $d \ln T_1/dP$, and dT_0/dP can be found. These are tabulated in Table I.

The dielectric-constant-vs-pressure data from sample II were treated in the following way. At each temperature, $1/\epsilon$ (see Fig. 3) was found to be linearly proportional to pressure, so that $d\epsilon^{-1}/dP$ is independent of pressure at least up to 3.5 kbar. Our measured value of $d\epsilon^{-1}/dP$ at room temperature is $7.6 \times 10^{-5}/kbar$, which agrees closely with the value of $8.1 \times 10^{-5}/kbar$ measured by Wemple *et al.*¹² If ϵ is described by Eq. (2), then

$$\frac{d\epsilon^{-1}}{dP}(T) = -\frac{1}{\epsilon} \left(1 - \frac{A}{\epsilon} \right) \frac{d \ln B}{dP} + \frac{(1/\epsilon)(1-A/\epsilon)}{\frac{1}{2} T_1 \coth(T_1/2T) - T_0} \left\{ \left[\frac{1}{2} \coth \frac{T_1}{2T} + \frac{1}{4} \frac{T_1}{T} \left(1 - \coth^2 \frac{T_1}{2T} \right) \right] \frac{dT_1}{dP} - \frac{dT_0}{dP} \right\} \quad (3)$$

In order to find $d \ln B/dP$, $d \ln T_1/dP$, and dT_0/dP from the $d\epsilon^{-1}/dP$, let us form from Eq. 3 the following expression:

$$\left\{ \frac{(\frac{1}{2} T_1 - T_0)\epsilon(0)}{[1 - A/\epsilon(0)]} \frac{d\epsilon^{-1}}{dP}(0) - \frac{[\frac{1}{2} T_1 \coth(T_1/2T) - T_0]\epsilon(T)}{[1 - A/\epsilon(T)]} \frac{d\epsilon^{-1}}{dP}(T) \right\} \left(\frac{1}{2} T_1 \coth \frac{T_1}{2T} - \frac{1}{2} T_1 \right)^{-1} \\ = \frac{d \ln B}{dP} + \left(\frac{1 + \coth(T_1/2T)}{2T} - \frac{1}{T_1} \right) \frac{dT_1}{dP} \quad (4)$$

If the zero-pressure values for the parameters A , B , T_1 , and T_0 are used, then the left-hand side consists only of measured quantities and is a function of temperature only. This analysis assumes that ϵ fits Eq. (2) to zero temperature. If this is so, then ϵ is very nearly temperature independent below 4 K, and the quantities evaluated at $T=0$ can equally well be evaluated at 4 K. Let us denote the left-hand side by $F(T)$. Then a plot of $F(T)$ vs $\{[1 + \coth(T_1/2T)]/2T\} - 1/T_1$ should give a straight line with a slope dT_1/dP and intercept $d \ln B/dP$. The data from sample II are plotted in this way in Fig. 4. Equation (3) evaluated at $T=0$ then gives

$$\frac{dT_0}{dP} = \frac{1}{2} \frac{dT_1}{dP} - (\frac{1}{2} T_1 - T_0) \frac{d \ln B}{dP} \\ - (\frac{1}{2} T_1 - T_0) \frac{\epsilon(0)}{[1 - A/\epsilon(0)]} \frac{d\epsilon^{-1}}{dP}(0) \quad (5)$$

The values for $d \ln B/dP$, $d \ln T_1/dP$, and dT_0/dP thus found are also shown in Table I. As can be seen from Table I, the agreement between the measurements on the two different samples is quite good, with the possible exception of the value of $d \ln T_1/dP$. The determination of $d \ln T_1/dP$ is quite sensitive to the measured value of $d\epsilon^{-1}/dP(0)$, and the indicated error limits correspond to a 2%

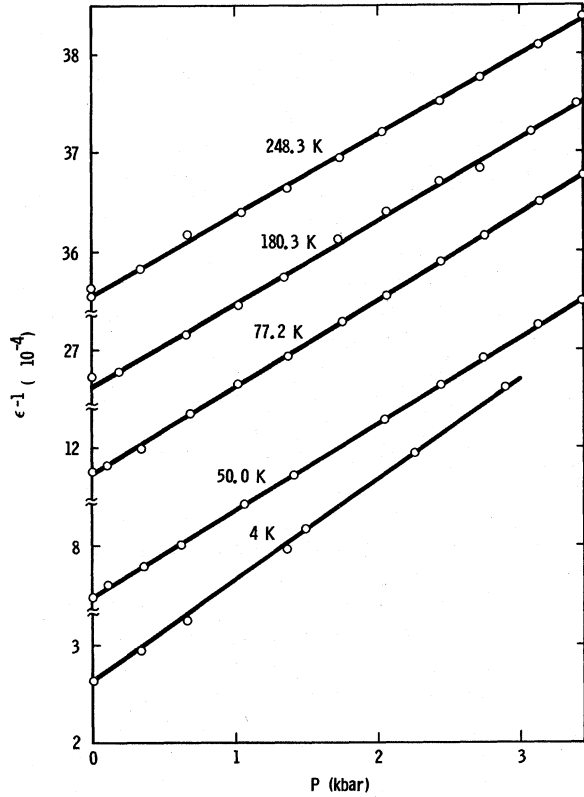


FIG. 3. Representative data for the inverse dielectric constant of sample II vs pressure, taken in the helium-gas apparatus at constant temperature.

error in $d\epsilon^{-1}/dP(0)$. This agreement indicates that nonhydrostatic effects in the piston-cylinder device are not important. The values obtained for $d \ln B/dP$ and dT_0/dP are similar to those found in other perovskite ferroelectrics. For example, in BaTiO_3 , $d \ln B/dP \approx -1\%/kbar$ and $dT_0/dP = -4.5 \text{ K/kbar}$.⁵

The static dielectric properties of the perovskites can be understood in terms of a soft ferroelectric ($q=0$, TO) mode. This soft ferroelectric mode has been studied by inelastic-neutron-scattering techniques.¹³ The square of the soft-mode frequency was found to follow closely the temperature dependence of ϵ^{-1} from 15 to 300 K. It might also be expected to follow the pressure dependence of ϵ^{-1} . The mode Grüneisen parameter γ may be found for the ferroelectric mode from $d\epsilon^{-1}/dP$. The definition of γ is $\gamma = -d \ln \omega_f / d \ln V$, where ω_f is the mode frequency and V is the volume. Since $\omega_f^2 \propto \epsilon^{-1}$, it follows that $\gamma = \frac{1}{2}(\epsilon/\kappa)(d\epsilon^{-1}/dP)$, where $\kappa = -d \ln V/dP$ is the volume compressibility. At 4 K and $P=0$, our results give $\gamma = 380$ for the ferroelectric mode. The data in Figs. 1 and 3 reflect variation of ω_f^2 with pressure (except for a scaling factor).

Although there have been more recent lattice-dynamical treatments of the low-temperature dielectric constant,^{14,15} Eq. (1) from Barrett,⁴ is apparently the only simple analytic expression derived to describe the low-temperature behavior. Barrett's theory does describe the observed temperature dependence of ϵ , but, as we shall see, predicts relations between the pressure derivatives which are inconsistent with our measurements. Barrett's model consists of independent ions (Ta in our case) in potentials of the form

$$\phi(r) = ar^2 + br^4, \quad (6)$$

where r is the displacement of the ion from its equilibrium position and a and b are constants. He uses the fourth-power term as a perturbation to the energies of a simple harmonic oscillator. The energy of the lowest level is kT_1 , and T_0 and B are derived in terms of a and b . From his results it is easy to show that the following relation should hold:

$$\frac{dT_0}{dP} = T_0 \frac{d \ln B}{dP} - \frac{2B}{C} \frac{d \ln T_1}{dP}, \quad (7)$$

where C is a model-dependent constant, but is probably between 1 and 10. Clearly, the second term on the right-hand side dominates since B is on the order of $5 \times 10^4 \text{ K}$ and T_0 is on the order of 10 K. Hence, we have

$$\left| \frac{dT_0}{dP} \right| > \sim 300 \text{ K/kbar}. \quad (8)$$

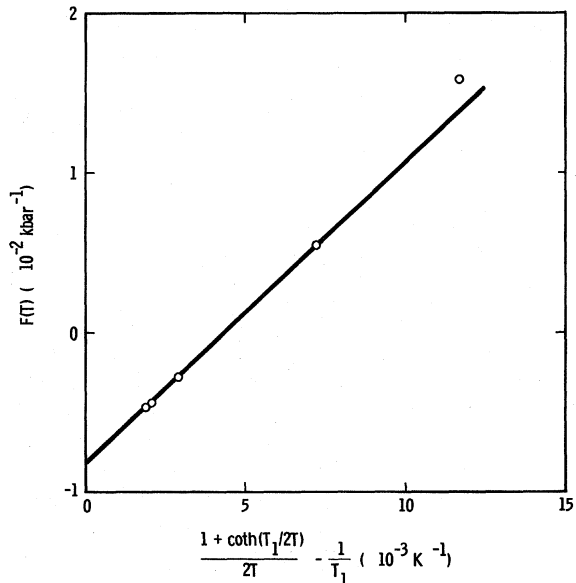


FIG. 4. $F(T)$ is a measured quantity defined in the text. The slope of the line gives dT_1/dP and the intercept gives $d \ln B/dP$.

We measure $dT_0/dP \sim -5$ K/kbar.

Barrett's model predicts the correct sign for $d \ln T_1/dP$. As the volume is decreased, the nearest neighbors of the ion would confine it to a smaller volume, thus raising the energy of the lowest quantum level, and hence T_1 . However, as pointed out above, either the measured value of $d \ln T_1/dP$ is too large, or that for $|dT_0/dP|$ is too small, to be consistent with Eq. (8). Since dT_0/dP is similar

to that measured for other perovskites, one might conclude that $d \ln T_1/dP$ is anomalous and that T_1 is not understood theoretically. Clearly more theoretical work is required.

ACKNOWLEDGMENTS

I would like to thank G. A. Samara for suggesting this problem. Steve Peerman and Gary Clendenen deserve much credit for making the measurements.

†Work supported by the U.S. AEC.

¹J. K. Hulm, Proc. Phys. Soc. (London) **A63**, 1184 (1950).

²J. K. Hulm, B. T. Matthias, and E. A. Long, Phys. Rev. **79**, 885 (1949).

³J. C. Slater, Phys. Rev. **78**, 748 (1950).

⁴J. H. Barrett, Phys. Rev. **86**, 118 (1952).

⁵G. A. Samara, in *Advances in High Pressure Research*, edited by R. S. Bradley (Academic, New York, 1969), Vol. 3, Chap. 3.

⁶T. Sakudo and H. Unoki, Phys. Rev. Letters **26**, 851 (1971).

⁷Obtained from Electro-Optical Division, Sanders Assoc., 95 Canal, Nashua, N. H.

⁸D. N. Lyon, D. B. McWhan, and A. L. Stevens, Rev. Sci. Instr. **38**, 1234 (1967).

⁹J. E. Schirber, Cryogenics **10**, 418 (1970). The apparatus used was constructed by L. R. Edwards of this laboratory.

¹⁰J. S. Dugdale, Nuovo Cimento Suppl. **9**, 27 (1958).

¹¹S. H. Wemple, Phys. Rev. **137**, A1575 (1965).

¹²S. H. Wemple, A. Jayaraman, and M. DiDomenico, Jr., Phys. Rev. Letters **17**, 142 (1966).

¹³G. Shirane, R. Nathans, and V. J. Minkiewicz, Phys. Rev. **157**, 396 (1967).

¹⁴R. A. Cowley, Phil. Mag. **11**, 673 (1965).

¹⁵N. S. Gillis and T. R. Koehler Phys. Rev. B (to be published).

Electronic Defect Structure of Single-Crystal ThO₂ by Thermoluminescence

Elward T. Rodine*

Systems Research Laboratories, Inc., Dayton, Ohio 45440

and

Peter L. Land

Aerospace Research Laboratories, Wright-Patterson AFB, Ohio 45433

(Received 18 January 1971)

Some electronic defects and the associated photoelectronic processes in ThO₂ are analyzed by utilizing the data from thermoluminescence (TL) and EPR measurements on a number of rare-earth-doped and undoped single crystals from various sources. (The EPR measurements were made by others.) Some fluorescence and absorption measurements are also utilized. Some TL glow peaks in the undoped ThO₂ correlate with the annealing of EPR spectra which are associated with trapped electrons. The similarity of glow curves for different crystals, the lack of hyperfine EPR structure, and the dependence on rare-earth doping suggests that some of the major electron traps are associated with oxygen vacancies, which may be complexed. The TL and EPR were induced by uv excitation, which created electrons and holes which are trapped. Some of the hole traps are identified as rare-earth ions in cubic sites. The rare earths provide all of the TL and fluorescence observed in Li₂O · 2WO₃ flux-grown ThO₂, and the total TL at saturation depends on the doping level. The TL excitation spectra and optical absorption measurements on Li₂O · 2WO₃ flux-grown undoped thoria indicate a band gap of 5.75 eV which is larger than previously reported. The thermal activation energies are given for electron traps, and some indications of relative cross sections for electron or hole trapping or recombination processes are reported.

INTRODUCTION

We have measured the thermoluminescence (TL) from a large number of ThO₂ single crystals. The crystals represent several different methods of

growth and have a wide variation of impurity content that includes intentional rare-earth doping. This paper deals primarily with the results and conclusions derived from the measurements on one group of crystals. More detailed data on these